ELSEVIER

Chemical Engineering Journal 79 (2000) 145–153

Chemical Engineering Journal

www.elsevier.com/locate/cej

Overall pressure balance and system stability in a liquid–solid circulating fluidized bed

Ying Zheng, Jing-Xu (Jesse) Zhu*

Department of Chemical and Biochemical Engineering, University of Western Ontario, London, Ont., Canada N6A 5B9

Received 22 May 1999; received in revised form 7 March 2000; accepted 3 April 2000

Abstract

A pressure balance analysis has been carried out, along with a dimensionless empirical correlation for the solids holdup in the riser and a semi-empirical equation for the pressure drop across the non-mechanical control valve derived in this work, to successfully predict the stable operating conditions and explain the origin of the unstable operation phenomena of the liquid–solid circulating fluidized bed. The effects of the total and auxiliary liquid velocity, the solids inventory and the unit geometry on the stable operation range are discussed. Furthermore, this work also reveals the importance of unit structure in improving the performance of the liquid–solid circulating fluidized bed systems.

Keywords: Pressure balance; Operation window; Maximum solids circulation rate; Circulating fluidized bed; Liquid–solids fluidization

1. Introduction

New processes in biochemical technology, water treatment, petroleum and metallurgical industries, etc. have led to the need for new types of liquid–solid contacting equipment. One of these is the liquid–solid circulating fluidized bed (LSCFB) in which the solid particles are entrained up in the riser, collected at the riser top and recirculated through a particle storage vessel back to the bottom of the riser. The flow characteristics in the riser were reported to be very uniform and the LSCFB is considered to be superior to the conventional liquid–solid fluidized bed given the improved liquid–solids contact and the increased liquid flowrate [1,2].

However, the operation of the LSCFB system may become unstable under certain operating conditions and it is very important to understand this phenomenon. The stable operation range of the LSCFB system was studied by Zheng et al. [2]. They observed unstable operation at higher solids circulation rates, when particles collected by the liquid–solid separator cannot be recirculated back quickly enough to the bottom of the riser to catch up with the increased solids circulating rate. When this happens, reducing either the total liquid or the auxiliary liquid flow rate would end the unstable operation. Furthermore, the stable operating range was found to be strongly affected by the feeding system. With higher static bed height in the particle storage vessel (i.e. higher solids inventory), the stable operation range is increased and higher solids circulation rate can also be reached without inducing unstable operation.

In the literature, different types of unstable operations have already been identified in the gas–solid vertical cocurrent upflow system. The so-called "choking" point, characterized by the formation of slugs and severe instability in the system, was first defined by Zenz and Othmer [3] as the starting point of unstable operation with decreasing gas velocity. Recently, instability resulting from pressure imbalance between the riser and the solids return side, was also observed in a gas–solid circulating fluidized bed system. This unstable state may occur prior to the choking point (i.e. at a higher gas velocity than the choking velocity) [4,5]. This instability was explained by the pressure balance between the riser and the downcomer [6,7]. However, no work has been reported for liquid–solid systems.

In this paper, an analysis of pressure balance in the whole loop is, for the first time, carried out for the LSCFB system to elucidate the origin of possible flow instability. This analysis is based on the overall pressure balance in the whole circulation loop, incorporating liquid and solid material balance on the total solids inventory. This allows one to evaluate the effect of operating conditions on the steady-state hydrodynamics. With the guidance of this analysis, it is possible to avoid operation instability due to the inappropriate pressure balance between the riser and the storage vessel and to allow a

* Corresponding author. Tel.: +1-519-661-2131; fax: +1-519-661-3498.
E-mail address: zhu@uwo.ca (J.-X. Zhu)

1385-8947/00/$ – see front matter
PII: S1385-8947(00)00168-6

circulating fluidized bed to operate at much higher solids circulation rates so that the stable operating range is enlarged.

In addition, a model describing the pressure drop across the control device and an empirical correlation to calculate the solids holdup in the riser have been proposed. The characteristics and the working principle of the non-mechanical valve in the liquid–solid system have also been discussed in detail.

2. Model development

2.1. Pressure balance in the system

The LSCFB consists of four main components: a riser, a storage vessel, a liquid–solid separator and a solids flow control device (Fig. 1). A simplified schematic of the liquid–solid system for pressure analysis is shown in Fig. 2. In such a system, a pressure loop forms when the particles are fluidized [7,8].

The pressure drop in the riser is composed of the liquid and solids static heads, the pressure drop due to solids acceleration (ΔP_{ac}), and the friction between the liquid and solids flow and the column wall (ΔP_{fs}). Since the fluidization velocity is not very high and the solids acceleration is very easy, the pressure drops due to solids acceleration and wall friction are not significant in the riser of the liquid–solid circulating system. Taking the pressure at the outlet of the liquid–solid separator as zero and excluding the pressure loss due to acceleration and friction, the pressure head at the bottom of the riser, P_r, can be calculated by

$$P_r = \rho_s(1-\varepsilon)gH + \rho_l\varepsilon gH \quad (1)$$

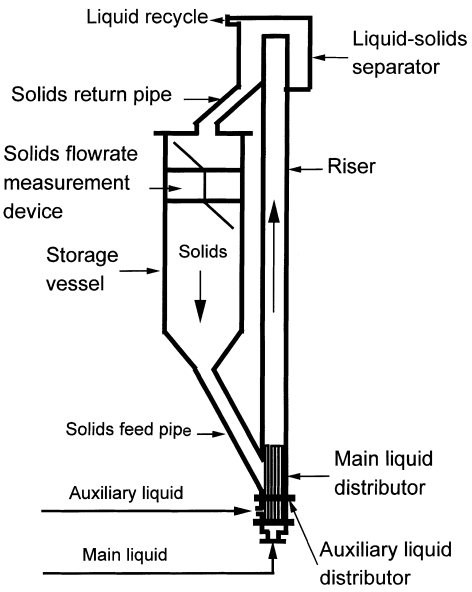

Fig. 1. The experimental LSCFB apparatus.

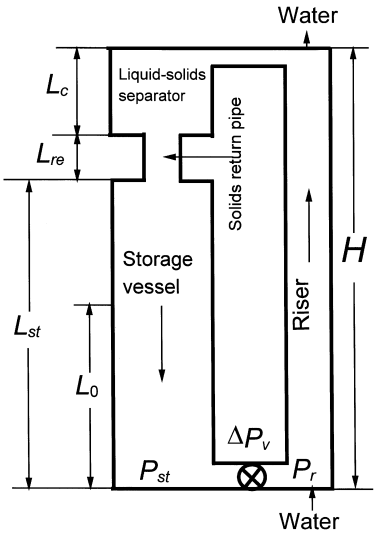

Fig. 2. Simplified LSCFB system.

In LSCFB systems, particles are carried up to the top of the riser, separated from the liquid by a liquid–solid separator and then returned back to the storage vessel through the returning pipe to form a slow-moving packed bed. For such a case, the solids acceleration and friction in the storage vessel can also be reasonably neglected. If the static bed height in the storage vessel is L_0 before fluidization (i.e. when all particles are stored in the storage vessel), the actual bed height in the storage vessel when the system is running, L_0', should be lower than L_0. The pressure head at the bottom of the storage, P_{st}, is caused by the pressure drops of the liquid–solid separator (ΔP_c), the returning pipe (ΔP_{re}), the section above the static bed (ΔP_{ds}) and the reduced solids inventory:

$$P_{st} = \rho_s(1-\varepsilon_{mf})gL_0' + \rho_l\varepsilon_{mf}gL_0' + \Delta P_{re} + \Delta P_c + \Delta P_{ds} \quad (2)$$

Particles separated by the liquid–solid separator fall back to the storage vessel through the return pipe by gravity. Since the diameter of the liquid–solid separator is close to that of the storage vessel, the suspension densities of both the separator and the section above the dense phase surface in the storage can be reasonably approximated as the same, i.e. $\varepsilon_c = \varepsilon_{ds}$. Assuming that the solids downflow velocity equals the particle terminal velocity, the voidage in the returning pipe ($1-\varepsilon_{re}$), and the voidage in the separator and the region above the dense phase surface and the separator ($1-\varepsilon_{ds}$) can be estimated by

$$1-\varepsilon_{re} = \frac{(D_r/D_{re})^2 G_s}{\rho_s U_t} \quad (3)$$

$$1-\varepsilon_c = 1-\varepsilon_{ds} = \frac{(D_r/D_{st})^2 G_s}{\rho_s U_t} \quad (4)$$

The pressure drops due to liquid and solids in those two regions can be calculated by

$$\Delta P_{re} = [\rho_l\varepsilon_{re} + \rho_s(1-\varepsilon_{re})]L_{re}g \quad (5)$$

$$\Delta P_c = [\rho_l \varepsilon_c + \rho_s(1-\varepsilon_c)]L_c g \quad (6)$$

$$\Delta P_{ds} = [\rho_l \varepsilon_{ds} + \rho_s(1-\varepsilon_{ds})](L_{st} - L_0')g \quad (7)$$

The total solids inventory is deducted by the solids holdups in the riser, the returning pipe, the liquid–solid separator and the region above the solids inventory:

$$L_0' = L_0 - \frac{D_r^2 H(1-\varepsilon) + D_{re}^2 L_{re}(1-\varepsilon_{re}) + D_{st}^2(L_{st} - L_0 + L_c)(1-\varepsilon_{ds})}{D_{st}^2(1-\varepsilon_{mf})} \quad (8)$$

When the solids holdup in the riser and the solids circulation rate (and therefore the superficial liquid velocity) are given, the pressure heads at the bottom of the storage vessel and the riser can be estimated by Eqs. (1)–(8).

2.2. A dimensionless empirical correlation for solids holdup in the riser

The solids holdup in the riser is affected by the operating conditions [2]: for a given total liquid velocity, solids holdup in the riser increases with increasing solids circulation rate; at a fixed solids circulation rate, however, an increase in liquid velocity leads to the decrease of solids holdup. When the operating conditions are set to the same, solids holdup may also be affected by the physical properties of both the particles and the fluid medium. An increase in the diameter and/or the density of the particles decreases the solids holdup under the same operating conditions [2]. Increasing the density and viscosity of the fluid is expected to decrease the suspension density in the riser, although there has not been experimental evidence to demonstrate this phenomenon. It is easy to understand the effect of the fluid density and viscosity from the interaction between the fluid medium and the solid particles since it is easier for dense and more viscous fluid to carry the solids up to the top of the riser.

For an ideal liquid–solid circulating fluidized system, where uniform spherical solid particles are employed, secondary variables such as distributor plate geometry, particle shape and particle size distribution need not be considered. A dimensionless empirical equation has been derived, in this paper, to correlate the solids holdup in a liquid–solid circulation fluidized bed system with the superficial liquid velocity and the solids circulation rate, based on glass beads and plastic beads reported by Zheng et al. [2]:

$$1 - \varepsilon = \frac{\overline{G}_s^{0.8}}{0.25\overline{U}_l^{1.9}} \quad (9)$$

where $\bar{G}_s$ is the dimensionless solids circulation rate and is defined as

$$\overline{G}_s = \frac{G_s}{(\mu g \Delta\rho\rho_l)^{1/3}} \quad (10)$$

and $\bar{U}_l$ is the dimensionless superficial liquid velocity defined as [9]

$$\overline{U}_l = U_l \left(\frac{\rho_l^2}{\mu g \Delta\rho}\right)^{1/3} \quad (11)$$

From Eqs. (9)–(11), it is seen that the bed voidage in the riser is mainly affected by the solids circulation rate, the liquid flow rate and the physical properties of particles and the fluidization media.

2.3. Pressure drop across the valve

The solids flow control devices can be divided into two main categories based on the way used to control the valve opening — mechanical and non-mechanical valves. Mechanical valves usually contain moving parts to control the valve opening mechanically. Since these devices rely on mechanical actuation, they are not commonly employed under high temperature and high pressure conditions in industrial processes because of their associated sealing and mechanical problems [10]. Non-mechanical valves, on the other hand, do not contain any moving parts but are controlled by the auxiliary fluid flow rate and the geometry of the pipe, and thus no sealing and/or mechanical problems are encountered at elevated temperatures and pressures [11].

The control device applied in this LSCFB belongs to the non-mechanical type. As shown in Fig. 1, it is located at the bottom of the riser and is comprised of the lift pot below the top of the main liquid distributor tubes, the solids feed pipe and the bend between the two. Before the auxiliary liquid flow is turned on, a packed bed is formed in the lift pot and no solids circulation occurs. When the auxiliary liquid flow is added, liquid flows upward through the particles and the relative liquid–solids movement produces a drag force on the particles in the direction of flow. When this drag force exceeds the force required to overcome the resistance to the solids moving through the constricting bend and the gravity of the particles, the solids begin to flow through the valve [12].

The quantity of solids passing through the valve is controlled by the auxiliary liquid flow rate. When the auxiliary liquid flow is completely closed, the particles in the storage vessel are unable to flow into the bottom of the riser because of the static friction between the liquid, the solids and the connecting bend. Thus, the valve can be considered completely closed and no continuous particle circulation could be achieved. Injecting the auxiliary liquid, the particles do not begin to flow immediately since the initial liquid flow added is not enough to produce the drag force required to start the solids flow. Only when a threshold liquid velocity is reached, the solids begin to flow. Above this threshold auxiliary liquid velocity, increasing liquid velocity causes the solids flow rate to increase and decreasing

the auxiliary liquid flow rate causes the solids flow rate to decrease.

Non-mechanical valves have been studied and a set of equations have also been developed to characterize the pressure drop across the valves for gas–solids flow [10,11]. However, no such equation is available for a liquid–solids system. The pressure drop across the valve for liquid–solids flow depends on the flow rate and the property of the liquid–solids mixture flowing through the valve and the construction of the valve. The more liquid–solid mixture that flows through the valve, the higher the pressure drop across the valve. Based on the various values of P_{st} and P_r, calculated from Eqs. (1) and (2), and the working principle of the non-mechanical valve, a correlation has been obtained here to best relate the pressure drop across the valve with the operating conditions for the water–glass beads system:

$$\Delta P_v = K \frac{G_{s,v}^{2.51}}{2[\rho_s(1-\varepsilon_{mf}) + \rho_l \varepsilon_{mf}]} \tag{12}$$

where K is the friction coefficient,

$$K = \frac{[\rho_s(1-\varepsilon_{mf}) + \rho_l \varepsilon_{mf}] g D_v}{0.125 U_a G_{s,v}} \tag{13}$$

and $G_{s,v}$ is the flux of the liquid–solids mixture through the valve assuming that the mixture has the same voidage as at minimum fluidization:

$$G_{s,v} = \left(1 + \frac{\rho_l \varepsilon_{mf}}{\rho_s(1-\varepsilon_{mf})}\right) \frac{W_s}{A_v} \tag{14}$$

Combining Eqs. (12) and (13), one has

$$\Delta P_v = \frac{G_{s,v}^{1.51} g D_v}{0.25 U_a} \tag{15}$$

Eq. (13) shows that the friction coefficient, K, decreases with increasing auxiliary liquid velocity. While Eq. (13) also implies that K decreases with increasing solids circulation rate, the pressure drop across the valve increases much faster with the solids circulation rate. As a result, the pressure drop across the valve increases with the solids circulation rate and decreases with the auxiliary liquid velocity, as given in Eq. (15).

2.4. Determination of steady operation window

In an LSCFB system, solids circulation rate and solids holdup in the riser under a fixed pair of U_l and U_a can be predicted by the equations proposed above with the following iteration procedure. For the given total and auxiliary liquid velocity, a solids circulation rate is first assumed. The average bed voidage is then calculated from Eq. (9). The calculated bed voidage and the assumed solids circulation rate are then substituted in Eqs. (1) and (2) to calculate P_r and P_{st}, respectively. At the same time, the pressure drop across the valve, ΔP_v, can be calculated from Eqs. (14) and (15) by the given auxiliary liquid velocity and the assumed solids circulation rate. If the value of ΔP_v is different from that of $P_{st} - P_r$, a new solids circulation rate for the same pair of U_l and U_a is assumed again to repeat the calculation until the two values fall within a pre-set error range. This solids circulation rate is then taken as the circulation rate corresponding to a given pair of auxiliary and total liquid velocities under steady state. If no possible solids circulation rate can be found to make the two values equal, an unsteady operation is reached. When the LSCFB system operates under unsteady state, the rate of particles returning back to the storage vessel cannot catch up with the increased solids circulation rate, i.e. the quantity of particles carried up to the top of the riser and separated by the liquid–solid separator are more than those falling back to the storage vessel. The solids circulation rate at the boundary of the stable and the unstable operation is the maximum/minimum solids circulation rate for the stable/unstable operation of this system. Beyond this solids circulating rate, the liquid–solids circulating fluidized bed cannot be operated at steady state.

3. Experiments

Experimental data were collected in the LSCFB system corresponding to the configuration in Fig. 1. The system consists of a Plexiglass riser column of 7.6 cm i.d. and 2.7 m in height, a storage vessel of 20.3 cm i.d. serving as solids reservoir, and a liquid–solid separator.

Liquid pumped from a liquid reservoir is divided into two streams with the main flow entering the main liquid distributor and the other going to the auxiliary liquid distributor. The function of the main liquid flow is to carry particles up to the top of the riser where the liquid–solid mixture is separated by the liquid–solid separator. Liquid is then returned to the liquid reservoir while the particles are returned to the particle storage vessel. The solids feeding system of this unit is controlled by the auxiliary liquid flow as discussed previously. When the auxiliary liquid flow is set to zero or below a threshold level, no particles in the storage vessel can enter into the riser and therefore no continuous solids circulation can be achieved. With increasing auxiliary liquid flow rate, more particles enter into the bottom of the riser and the column becomes denser.

Liquid flows were metered by rotameters. The solids circulation rate was determined by measuring the accumulated solids for a known period of time in the top section of the storage vessel. The solids circulation measurement device contains two half columns as shown in Fig. 1 so that it does not affect the solids circulation rate [2]. The pressure drops were recorded using manometers attached to eight pressure taps located along the riser column. Glass beads with a mean diameter of 508 μm and a density of 2490 kg/m^3 were used. All experiments were carried out at ambient temperature and tap water was used as the fluidizing liquid. During each experiment, both the main liquid flow and the auxiliary liquid flow were adjusted carefully until the

whole system operated in a stable steady-state manner, with a constant solids circulation rate.

4. Validation of the model

The semi-empirical equations (12)–(15) are used to predict the pressure drop across the valve, ΔP_v. This value is then compared with the value of $P_{st}-P_r$, calculated by Eqs. (1) and (2) with the given U_l, G_s and the experimentally measured ε_s to verify those equations. The calculated ΔP_v, as mentioned above, should balance $P_{st}-P_r$ when the LSCFB operates under a steady state. Fig. 3 shows the calculated $P_{st}-P_r$ based on experimentally obtained ε_s and the predictions for the variations of the pressure drop across the valve with the solids circulation rate and the auxiliary liquid flow. Both the magnitude and the trends of the predictions are seen to be in good agreement with almost all the data to within ±10%. In Fig. 3, it is seen that the pressure drop across the valve always increases with increasing solids circulation rate at a fixed secondary liquid flow rate but decreases with increasing auxiliary liquid flow rate for a given solids circulation rate. With an increase in the solids circulation rate, more particles flow through the valve, leading to an increase of the friction between the liquid–solid mixture and the valve, and thus increasing the pressure drop across the valve. On the other hand, the auxiliary liquid flow rate changes the friction and works like an "opening area" controller of the valve. Increasing the auxiliary liquid velocity, the "opening" of the valve is "enlarged" due to reduced friction. When the solids circulation rate remains the same, the pressure drop across the valve should decrease with increasing auxiliary liquid flow according to Eq. (15). For each given solids inventory (expressed as the initial static bed height), Fig. 4 shows that the increase of the pressure drop with the solids circulation rate has the same trend and that the static bed height has little influence on ΔP_v.

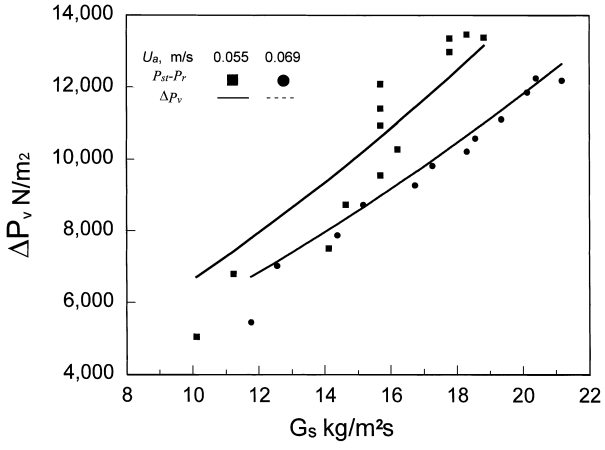

Fig. 3. Comparison of model predications for the pressure drop across the valve with the calculated $P_{st}-P_r$ based on experimental data with L_0=1.5 m.

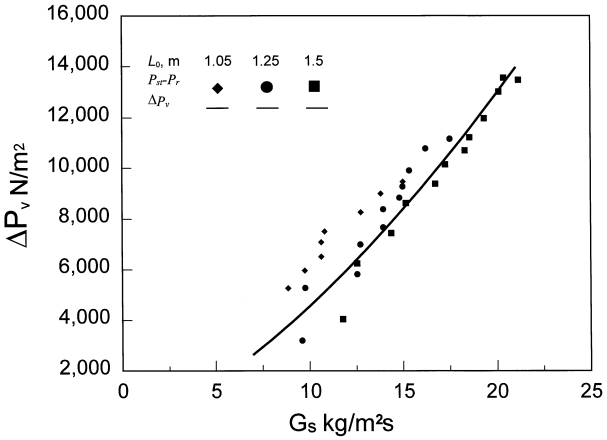

Fig. 4. Comparison of model predications for the pressure drop across the valve with the calculated $P_{st}-P_r$ based on experimental data with three different solids inventory heights under U_{l_2}=0.069 m/s.

However, the range of the pressure drop is larger for higher static bed height as implicated in Fig. 4. Under the same operating conditions, more solids inventory leads to a higher maximum solids circulation rate under the steady state and therefore a wider range of the pressure drop across the valve.

Fig. 5 shows the predicted and the measured solids holdup with different solids inventory. The predicted average solids holdup in the riser is calculated by Eq. (9) in conjunction with Eqs. (10) and (11) based on the given liquid velocity and solids circulation rate. Good agreement is obtained. This agreement clearly shows the validity of Eq. (9). Fig. 5 also indicates that the liquid flow rate and solids circulation rate are the main factors which influence the solids holdup in the riser: the solids holdup is increased with increasing solids circulation rate but with decreasing liquid flow rate. Comparing Fig. 5a and b, it is seen that the variations of solids holdup under the two levels of the static bed heights follow the same trend, suggesting that the feeding system does not affect the flow characteristics of the LSCFB system.

When the LSCFB is operated at steady state, both the solids holdup in the riser and the solids circulation rate for a given pair of total and auxiliary liquid flow rates can be predicted by the pressure balance analysis: the pressure drop across the valve must equal the pressure drop between P_{st} and P_r for a stable operation. Following the calculation procedure given in the previous section, the predictions for the solids holdup and the solids circulation rate in the riser are compared with the experimental data in Fig. 6. Good agreement is obtained. This agreement confirms that the operating state of the LSCFB is controlled by the pressure balance in the unit and our pressure balance analysis works very well.

5. Conditions for stable operation

For the LSCFB system shown in Fig. 1, the total solids inventory in the whole system expressed as the initial static

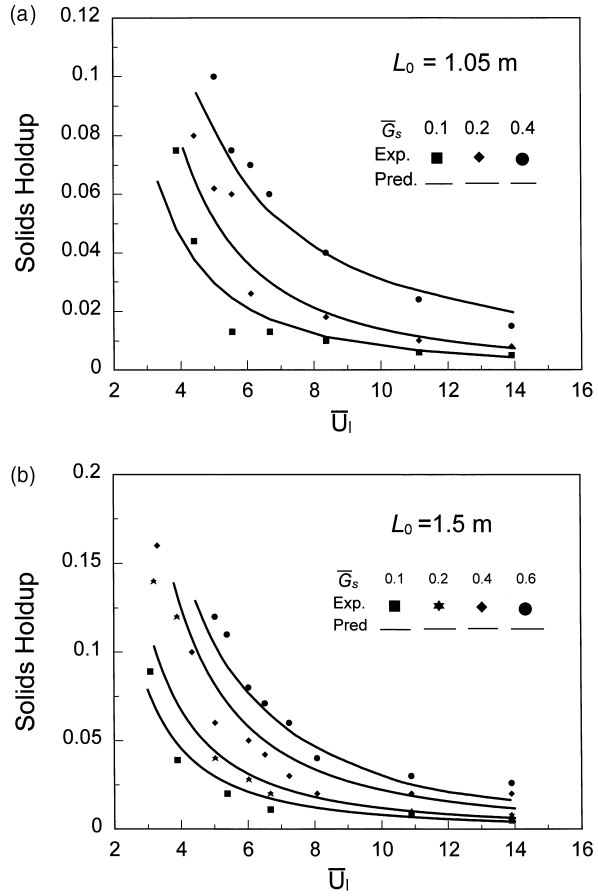

Fig. 5. Comparison of model predications with experimentally obtained solids holdup in the riser at different dimensionless solids circulation rates for: (a) L_0=1.05 m; and (b) L_0=1.50 m.

bed height in the storage tank is L_0 and there is no solids addition to or removal from the system during the operation. With high enough total and auxiliary liquid flow rates, particles can be circulated between the riser and the storage vessel. At a steady state, the solids circulation rate achieved in the riser balances the solids recirculation rate back to the storage vessel and an appropriate pressure balance in the entire loop is established. By increasing the auxiliary liquid flow rate, more particles are allowed to enter into the bottom of the riser and the solids circulation rate is increased. Eventually, a point will be reached when the solids circulation rate achieved in the riser is higher than the solids flow rate returned back to the storage vessel. At this point, the appropriate pressure balance in the unit is broken and an unstable operation state is reached.

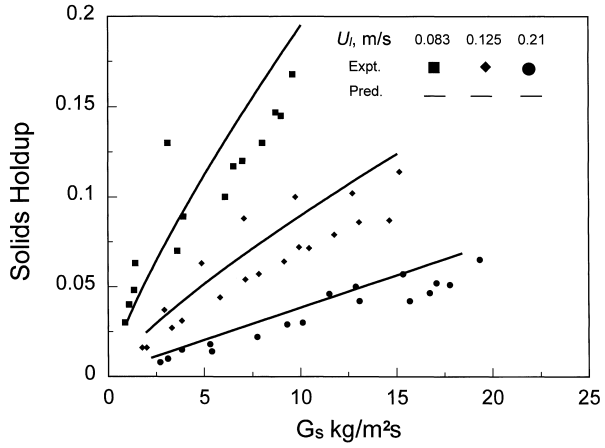

Fig. 6. Comparison of model predications with experimental data at different operating conditions.

To sustain a steady-state operation, an appropriate pressure balance in the unit needs to be maintained, i.e. $P_{st}-P_r=\Delta P_v$. Adjusting the operating conditions, the system will first disturb the balance and then attains steady operation after a transient period when the solids circulation rate varies. For a given auxiliary liquid flow rate, the solids circulation rate/solids holdup first increases/decreases quickly with increasing total liquid flow rate and then the increasing/decreasing of the solids circulation rate/solids holdup becomes insignificant [2]. Under this operating condition, an increase in the total liquid velocity will cause a reduction of P_r and an increase of ΔP_v due to the decrease of solids holdup in the riser and the increase of the solids circulation rate, respectively. The decrease of P_r with U_l and the increase of ΔP_v with G_s can be predicted by Eq. (1) and Eqs. (12)–(15), respectively. Meanwhile, this variation only leads to a minor decrease of solids inventory in the storage vessel because the diameter of the storage vessel is much larger than that of the riser. The small decrease of P_{st} and the obvious decrease of P_r eventually lead to a new pressure balance with an increased ΔP_v in the loop, at a higher solids circulation rate than before.

However, when the solids circulation rate is beyond a certain value, unstable operating conditions are attained when the solids recirculation rate cannot catch up with the increase of the solids circulation rate in the riser. This unstable operation may be explained as follows: the auxiliary liquid flow, U_a, is introduced right below the intersection of the riser and the solids feed pipe. With a relatively low flow rate, U_a flows mainly up into the riser due to the resistance of the particles packed in the solids feed pipe. When the auxiliary liquid flow rate is set high, it may split into two streams with one stream flowing up into the riser and the other one entering the solids feed pipe. The part of the auxiliary liquid flow entering the solids feed pipe flows up by going through the particles in the storage vessel, the returning pipe and then enters the liquid–solid separator. An increase in U_a leads to an increase of G_s, which in turn results in higher solids holdup in the riser and therefore a higher P_r. This relative increase of P_r to P_{st} allows a higher proportion of U_a to flow though the solids return side. This increased liquid stream creates more resistance to the particles in the liquid–solid separator from recirculating back to the storage vessel. When the solids circulation rate is beyond a certain value, particles transported up to the top of the riser are more than those returned back to the storage vessel. Particles are then stuck in the liquid–solid separator and the solids inventory height in the storage vessel

drops quickly. This causes pressure imbalance between the riser and the particle storage vessel, leading to an unstable operation of the system. Under such unstable flow conditions, more liquid will preferentially pass through the solids return side, and will eventually terminate the particle circulation. Therefore, under a given total liquid velocity, there is a maximum solids circulation rate, associated with a maximum U_a, beyond which the operation becomes unstable.

6. Discussion

The maximum solids circulation rate against a given pair of U_l and U_a can be predicted through the analysis of pressure balance in the whole loop (Eqs. (1), (2), (9) and (15)). Fig. 7 shows the predicted values of ΔP_v and $P_{st}-P_r$ for three levels of the static bed height when the auxiliary liquid velocity is 0.069 m/s. Under this high auxiliary liquid velocity, the maximum solids circulation rate can be reached with increasing the total liquid velocity. At relatively low total liquid velocity, where solids circulation rate is also low, it is seen that $P_{st}-P_r$ balances ΔP_v, suggesting that there is enough pressure available to maintain the solids circulation rate and the system is operated under steady state. Increasing liquid flow rate to increase the solids circulation rate, both ΔP_v and $P_{st}-P_r$ increase. Beyond a certain point, the increasing ΔP_v is higher than that of $P_{st}-P_r$, indicating that the proper pressure balance is broken. At that point, the maximum solids circulation rate under the steady operation is obtained. For example, when U_l>0.25 m/s (L_0=1.05 m, U_a=0.069 m/s), the "available" pressure, $P_{st}-P_r$, is not enough to overcome the pressure across the valve, P_r, so that the liquid velocity of 0.25 m/s demarcates the boundary of the unstable and stable operation.

From the foregoing analysis, it is noted that there exists a maximum solids circulation rate for a given pair of U_l and U_a. The operation of the LSCFB becomes unstable when the solids circulation rate is higher than the maximum. Thus, the operation window in terms of maximum solids circulation rate can be determined by similar plots as shown in Fig. 7. Those results over a wide range of U_a are given in Fig. 8. When the LSCFB operates in the area below the boundary, shown as a dotted line, stable operation is obtained. As discussed above, the auxiliary liquid velocity and the solids circulation rate are the two main operating factors to affect the stable operation range of the LSCFB. The auxiliary liquid flow rate determines the possibility of the unstable operation. At low auxiliary liquid velocity (e.g. U_a=0.25 m/s), the system is always operated in steady state due to the limited solids feeding so that the maximum stable liquid flow rate is only limited by pump capacity. Increasing the auxiliary liquid velocity, the risk to reach an unstable operation of the LSCFB increases. When the auxiliary liquid velocity is set high, the maximum solids circulation rate could be reached when the total liquid velocity in the riser column is increased. Therefore, the available operation range of the liquid velocity decreases with increasing auxiliary liquid velocity. For example, when the auxiliary liquid velocity reduces from 0.069 to 0.055 m/s, the available operation range of the liquid velocity increases from 0–0.25 to 0–0.32 m/s.

Fig. 8 also seems to indicate that there are two different regions within the stable operation window, with one for lower auxiliary flow rate and the other for higher auxiliary liquid flow rate. At lower U_a, solids circulation rate is low and it is not easy to reach a pressure imbalance so that the maximum stable operating liquid flow rate is only restricted by the pump capacity. At higher U_a, the unstable operation becomes possible and the boundary of the stable operation is demarcated by the maximum solids circulation rate. In this region, the available operation range of the liquid velocity is constrained by the maximum solids circulation rate (and thus the pressure balance).

Fig. 8 further shows that the solids circulation rate increases quickly with increasing liquid velocity at first and then the increase of the solids circulation rate reduces thereafter. This implies that solids circulation at higher U_l is more restricted by the solids feeding system. Additionally, the

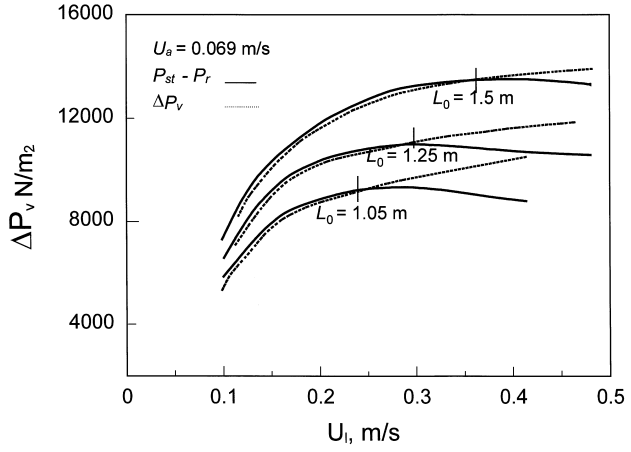

Fig. 7. Predicted values of ΔP_v and $P_{st}-P_r$ for three levels of the static bed height at U_{l_2}=0.069 m/s.

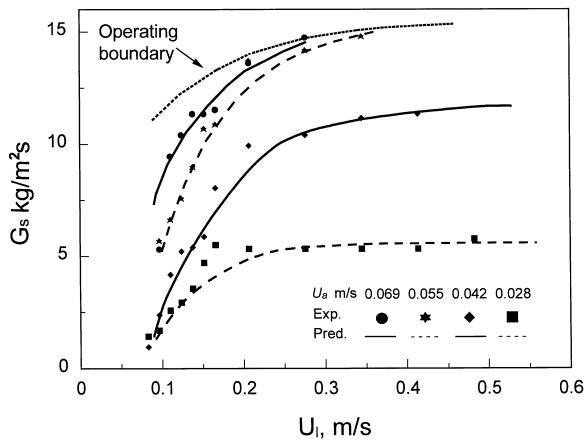

Fig. 8. Predicted stable operation range for L_0=1.05 m.

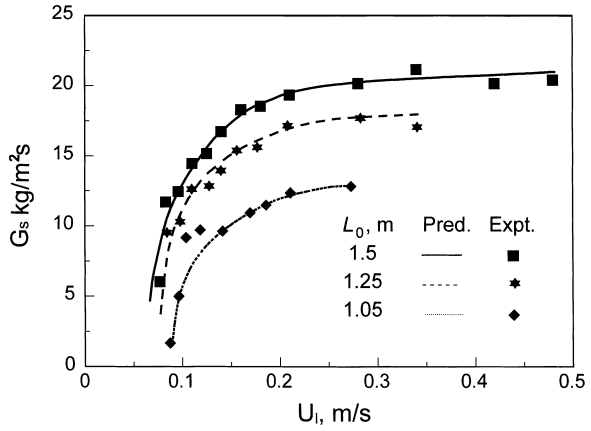

Fig. 9. Effect of the auxiliary liquid velocity on the stable operation range.

constant U_a curves in Fig. 8 are seen to converge with decreasing liquid velocity. This indicates that the solids circulation rate is less affected by the valve setting at low solids circulation rates. On the other hand, the valve provides an important regulation function at higher solids circulation rates. For a high liquid velocity, increasing the liquid velocity can only slightly increase the solids circulation rate because the solids circulation rate is no longer sensitive to the variation of the liquid velocity. To achieve higher solids circulation rates, a better measure is to increase the pressure head available for the solids feeding system by adding more particles to the storage vessel and/or reducing the pressure loss across the valve. As shown in Fig. 9, the solids circulation rate can reach a higher value with increasing solids inventory under the same operating conditions. For example, the maximum solids circulation rate for stable operation changes from 13 to 21 kg/m^2 s when the static bed height is increased from 1.05 to 1.5 m. This is expected since the increased solids inventory provides a higher pressure head at the bottom of the storage vessel, which increases the solids circulation rate and hence allows higher particle concentration in the riser, as reflected in Eqs. (1), (2) and (15).

The system geometry could be another important factor affecting the stable operating conditions in an LSCFB. Eqs. (1), (2), (13) and (14) show that the storage vessel-to-riser diameter ratio, the returning pipe-to-riser diameter ratio, the feeding pipe-to-riser diameter ratio, the static bed height in the storage vessel, and the riser height all play very important roles. However, there seems to be no experimental results to show the effects of these design parameters. More experiments are needed to achieve a better understanding of the appropriate operating conditions and of the influencing factors.

7. Conclusion

The analysis of the LSCFB system based on the pressure balance shows that the stable operation is built upon an appropriate pressure balance, $P_{st}-P_r=\Delta P_v$, in the whole circulation loop. The operating conditions of the system can greatly affect the pressure balance. The pressure head at the bottom of the riser, P_r, increases with increasing solids circulation rate but decreases with increasing total liquid velocity. On the other hand, the pressure head at the bottom of the storage vessel, P_{st}, varies insignificantly with the operation conditions due to the large storage vessel-to-riser diameter ratio. The solids circulation rate and the auxiliary liquid flow rate are the main operating parameters affecting the pressure drop across the non-mechanical control valve, ΔP_v, as given in Eq. (15). Under a stable operating state, $P_{st}-P_r$ will eventually balance ΔP_v after a transient period of disturbance when the operating condition is adjusted.

The pressure balance analysis shows that there exists a maximum solids circulation rate for a given auxiliary liquid velocity, beyond which a stable operation of the LSCFB system is not possible. At low auxiliary liquid flow rate, the system can always be operated under steady state since the solids circulation rate cannot be high enough to break the pressure balance built between the riser and the storage vessel. When the auxiliary liquid flow rate is set high, on the other hand, the maximum solids circulation rate can be reached with increasing total liquid velocity. Once the solids circulation rate is higher than the maximum, the available pressure drop, $P_{st}-P_r$, cannot overcome the pressure drop across the valve so that the appropriate pressure balance is broken and the stable operation cannot be maintained.

The model simulation further shows that the attainable maximum solids circulation rate and stable operation range are strongly influenced by the total solids inventory and the unit geometry. Higher solids inventory leads to higher available maximum solids circulation rates. To achieve higher solids circulation rate, sufficient back pressure needs to be provided at the bottom of the riser, by increasing the pressure buildup in the storage vessel.

8. Nomenclature

A_v	the cross-area of the feeding pipe (m^2)
D_r	riser diameter (m)
D_{re}	returning pipe diameter (m)
D_{st}	storage vessel diameter (m)
D_v	feeding pipe diameter (m)
g	acceleration due to gravity (m^2/s)
G_s	solids circulation rate (kg/m^2 s)
$G_{s,v}$	flux of liquid–solid mixture flowing through the valve (kg/m^2 s)
$\overline{G}_s$	dimensionless solids circulation rate, defined in Eq. (10)
H	riser height (m)
K	friction coefficient of the valve, as including the separator, defined in Eq. (13)
L_c	height of the liquid–solid separator (m)
L_0	static bed height in storage vessel (m)
L_0'	actual bed height in storage vessel (m)

L_{re} equivalent length of the returning pipe (m)
L_{st} height of the storage vessel (m)
P_r pressure head at the bottom of the riser (N/m^2)
P_{st} pressure head at the bottom of the storage vessel (N/m^2)
U_a superficial velocity of the auxiliary liquid flow (m/s)
U_l total superficial liquid velocity, including the auxiliary liquid flow (m/s)
$\overline{U}_l$ dimensionless superficial liquid velocity, defined in Eq. (11)
U_t terminal velocity of single particle (m/s)
W_s solids flow rate (kg/s)

Greek letters

ε average bed voidage
ε_c voidage in the liquid–solid separator
ε_{mf} voidage at minimum fluidization
ε_{re} voidage in the returning pipe
ε_{ds} voidage of the region above dense phase surface in the storage vessel
ε_s solids holdup
ρ_l density of liquid (kg/m^3)
ρ_s apparent density of solids (kg/m^3)
$\Delta\rho$ the density difference between solid and liquid (kg/m^3)
μ viscosity of liquid (kg/m s)
ΔP_c pressure loss through the liquid–solid separator (N/m^2)
ΔP_{ds} pressure drop over the liquid–solid mixture in the region above the actual bed in the storage vessel (N/m^2)
ΔP_{re} pressure head of the liquid–solid mixture in the returning pipe (N/m^2)
ΔP_v pressure loss across the solids control valve (N/m^2)

Acknowledgements

The financial support from the University of Western Ontario through the President Scholarship of Graduate Studies to the Ying Zheng is gratefully acknowledged.

References

[1] W.-G. Liang, S.-L. Zhang, J.-X. Zhu, Y. Jin, Z.-Q. Yu, Z.-W. Wang, Flow characteristics of the liquid–solid circulating fluidized bed, Powder Technol. 90 (1997) 95–102.
[2] Y. Zheng, J.-X. Zhu, J. Wen, S. Martin, A.S. Bassi, A. Margaritis, The axial hydrodynamic behavior in a liquid–solid circulating fluidized bed, Can. J. Chem. Eng. 77 (1999) 284–290.
[3] F.A. Zenz, L.H. Othmer, Fluidization and Fluid-particle Systems, Reinhold, New York, 1960.
[4] R. Bader, J. Findlay, T.M. Knowlton, Gas/solid flow patterns in a 30.5-cm-diameter circulating fluidized bed, in: P. Basu, J.F. Large (Eds.), Circulating Fluidized Bed Technology, Vol. II, Pergamon Press, Toronto, Ont., 1988, pp. 123–137.
[5] T. Hirama, H. Takeuchi, T. Chiba, Regime classification of macroscopic gas–solid flow in a circulating fluidized bed riser, Powder Technol. 70 (1992) 215.
[6] D. Bai, A.S. Issangya, J.-X. Zhu, J.R. Grace, Analysis of the overall pressure balance around a high-density circulating fluidized bed, Ind. Eng. Chem. Res. 36 (1997) 3898–3903.
[7] H.-T. Bi, J.-X. Zhu, Static instability analysis of circulating fluidized bed and the concept of high density risers, AIChE J. 39 (1993) 1272–1280.
[8] M.J. Rhodes, D. Geldart, A model for the circulating fluidized bed, Powder Technol. 53 (1987) 155–162.
[9] J.R. Grace, Contacting modes and behaviour classification of gas–solid and other two-phase suspensions, Can. J. Chem. Eng. 64 (1986) 353–363.
[10] L.S. Leung, Y.O. Chong, J. Lottes, Operation of V valves for gas–solid flow, Powder Technol. 49 (1987) 271–276.
[11] W.-C. Yang, T.M. Knowlton, L-valve equations, Powder Technol. 77 (1993) 49–54.
[12] T.M. Knowlton, Standpipes and return systems, in: J.R. Grace, A.A. Avidan, T.M. Knowlton (Eds.), Circulating Fluidized Beds, 1st Edition, Blackie, London, 1997, pp. 240–253 (Chapter 7).